# Spatiotemporal Pattern Generation using Frequency Dependent Chaos
# (Towards Tunable Evolution and Emergence)

Sai Venkatesh Balasubramanian

*Sree Sai Vidhya Mandhir, Mallasandra, Bengaluru-560109, Karnataka, India.*
*saivenkateshbalasubramanian@gmail.com*

## Abstract

A novel kind of chaos dependent on frequency and offering the twin advantages of easy tunability and simplicity of implementation is proposed, using which, a simple methodology to generate a chaotic signal is designed and implemented in hardware using FPGA, and the generated chaos is characterized using standard parameters such as Lyapunov Exponents and Kolmogorov Entropy. This temporal signal is used as the basis acting on a spatial propagation rule to generate spatiotemporal patterns. The generated patterns and their dependence on the spatial and temporal rules are studied. The distinguishing features of the obtained spatiotemporal patterns are simplicity of implementation, richness of features observed and a temporal rather than a spatial basis for generation, leading to implementation without employing memory consuming neighbourhood rules, which form the highlights of the present work. The generation of spatiotemporal patterns is seen as a road to tunable evolution and emergence, and finds immense applications such as bar code and random number generators.

*Keywords:* Spatiotemporal Patterns, Chaos Generation, Frequency Dependent Chaos

## 1. Introduction

As the flagship of Nonlinear Science, Chaos Theory has witnessed an exponential progress in recent years, thanks to the advancement of computing and storing power in recent years, coupled with the ability to simulate complex systems and visualize their long-term evolution patterns [1, 2]. The essence of chaos theory is determinism with an extremely sensitive dependence on initial conditions [3, 4, 5]. Chaos theory has had great success as a platform and tool to model and study various and diverse systems occurring in nature such as celestial mechanics, biological systems, chemical reactions, spread of epidemics, weather patterns and so on [4, 3, 6].

In electronics, the introduction of the Chua diode as a nonlinear element has enabled considerable progress in generating a wide variety of chaotic signals [5]. The generation of chaos electrically finds application in secure communication systems, showing great resistance to hacking, thanks to the sensitivity property of chaos, with related applications such as bar code generation and pseudo random number generation [7, 8].

The present work purports to the formulation and the generation of a frequency dependent chaos and the generation of spatiotemporal patterns using the generated chaotic signal as the basis [4, 6]. The advantages of frequency dependent chaos are twofold, as follows:

1. It builds on the basic premise that any signal can naturally be decomposed into a set of frequencies [9]. This leads to easy implementation using a single transistor as the chaotic 'system', since the nonlinearity proposed in the frequency dependant chaos is the natural switching operation of the transistor [9].
2. Having frequency as the control parameter makes it easy to tune the system, which enables a signal based control, a marked deviation from the system defined control typically seen in chaotic systems [4].

In the present work, an extremely simple method of generating frequency dependent chaos is described and the implementation is carried out in hardware using FPGA. The generated signal is characterized quantitatively using parameters such as Lyapunov Exponent, Kolmogorov entropy and Fractal Dimension and the dependence of the nature of chaos on frequency is studied. The generated 'temporal' signal forms the basis for the generation of spatiotemporal patterns according to a 'spatial rule' defined. The spatial patterns generated for different temporal and spatial control parameters are explored and a feature study is performed. The extremely simple method used for the generation of spatiotemporal patterns combined with the rich variety of patterns obtained form the principal highlights of the present work. The spatiotemporal patterns generated act as suitable bases for various applications such as bar code generators and random number generators.

## 2. Generation and Characterization of the Temporal Chaotic Signal

The formulation of frequency dependent chaos builds upon three crucial elements - a switching function, a frequency ratio and the waveform of the driving signal. Owing to the increased ubiquity of chaos in the square wave case, the driving waveforms in the present work are chosen as square waves. Two square waves given by $A(t)=square(f_1 t)$ and $B(t)=square(f_2 t)$ with frequencies $f_1$ and $f_2$ are the driving signals, with the controlling parameter given by $r=f_2/f_1$. By using a differential function $abs(A - B)$ for the switching nonlinearity, it is possible to represent the three key components of switch, ratio and waveform *ipso facto* into a single simple function, given as follows:

$$C(t) = mod(abs[square(f_1 t) - square(f_2 t)], \pi) \tag{1}$$

where $t$ denotes the temporal coordinate in samples. The nature of the chaotic signal $C(t)$ generated using the above relation heavily depends on the driving frequency ratio $r=f_2/f_1$. The above mentioned relation forms the basis for the spatiotemporal pattern generation and is implemented in hardware using the Altera Cyclone II-DE1 FPGA, with a base clock frequency of 50MHz. The required frequencies for $A(t)$ and $B(t)$ are obtained by dividing the clock frequency appropriately. The ratio is set to the irrational number $\pi$.

### 2.1. Characterization of the Chaotic Signal $C(t)$

The chaotic nature of the $c(t)$ is established by calculating the largest Lyapunov Exponent (LLE), a measure of a system's sensitive dependence on initial conditions [10, 11]. Rosenstein's algorithm is used to compute the Lyapunov Exponents $\lambda_i$ from the voltage waveform, where the sensitive dependence is characterized by the divergence samples $d_j(i)$ between nearest trajectories represented by $j$ given as follows, $C_j$ being a normalization constant: $d_j(i) = C_j e^{\lambda_i(i\delta t)}$. The Largest Lyapunov exponent thus obtained for the chaotic signal is 8.82, the positive value proving the fact that the signal is indeed chaotic.

The chaotic/fractal nature of the signal is further confirmed by computing the fractal dimension, using the Minkowski Bouligand Box Counting Method [12]. In this method, various square 'boxes' of different sizes $e$ are formed and for each size $e$, the number of boxes $N(e)$ required to cover the entire set is computed [12]. The fractal dimension $D$ is then given by $D = \lim_{e \to 0} \frac{log(N(e))}{log(e)}$. For the generated signal, the fractal dimension is obtained as 0.661, indicating the presence of self-similarity in the generated signal.

Finally, the worthiness of the generated signal as a potential candidate as a carrier of information can be established by ascertaining the amount of information that can be carried by the signal. This is precisely quantified by the Kolmogorov Entropy, a statistical measure of the uncertainty of the signal [10, 8, 1]. By assigning each of the $N$ quantifiable states of the amplitude of the output signal as an event $i$, the Kolmogorov Entropy $K_2$ obtained depends on their probabilities $p_i$ according to the relation $K_2 = - \sum_{i=1}^{N} p_i \log p_i$. The $K_2$ value is obtained as 6.79 bits/symbol, clearly testifying to the information carrying capacity of the generated chaotic signal.

### 2.2. Effect of Frequency Ratio on the nature of chaos

In order to ascertain the effect of the driving frequency ratio of the nature of the chaos generated, the values of $LLE$, $D$ and $K_2$ are recorded for frequency ratios between 1 and 2 in steps of 0.1 and are tabulated in Table 1.

Table 1: Effect of Driving Signal Frequency on the Generated Chaos

| Frequency Ratio $r$ | $LLE$ | $D$ | $K_2$ (bits/sym) |
|---|---|---|---|
| 1.1 | 8.18 | 0.661 | 6.67 |
| 1.2 | 8.01 | 0.67 | 6.92 |
| 1.3 | 8.84 | 0.665 | 6.87 |
| 1.4 | 8.57 | 0.662 | 6.81 |
| 1.5 | 8.17 | 0.661 | 6.77 |
| 1.6 | 8.21 | 0.661 | 6.79 |
| 1.7 | 8.89 | 0.665 | 6.88 |
| 1.8 | 8.66 | 0.662 | 6.82 |
| 1.9 | 8.12 | 0.661 | 6.73 |

From the Table, it is clearly seen that the driving signal frequency ratio does have a significant effect on the nature of the chaos generated. On this basis, the frequency ratio used shall be termed the 'temporal rule'.

## 3. Generation and Characterization of Spatio-Temporal Patterns

The generated temporal chaotic signal $C(t)$ is used as the basis for generating spatiotemporal patterns. Specifically, an N-celled system is taken and for the $i-th$ cell in the system, a 'spatial rule' deriving the cell output $C(i)$ from the previous cell outputs are defined. The spatial rule used in the present work is given as follows:

$$C(i) = mod(abs[C(i-1) - C(i-1-Nfactor)], \pi) \tag{2}$$

where the spatial coordinate $i$ ranges from 3 to N. This relation is not defined for the first two cells ($i = 1, 2$) and thus, these cells are defined to be the 'originators'. Thus, two temporal signals are generated and used as the originators. An interesting property of the 'spatial rule' is the $Nfactor$ parameter. As will be seen in the forthcoming discussion, this $Nfactor$ determines the nature of the spatiotemporal pattern generated. A block diagram illustrating the spatiotemporal pattern generation combining the temporal and spatial rules is shown in Fig. (1), along with the FPGA implementation setup and details of the components used in Fig. (2).
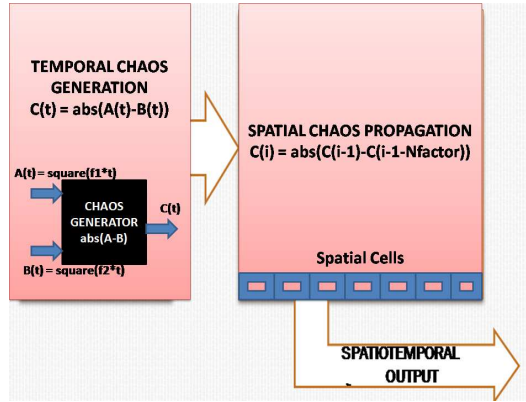


Figure 1: Block Diagram of the proposed spatiotemporal pattern generator illustrating the spatial and temporal 'rules'.
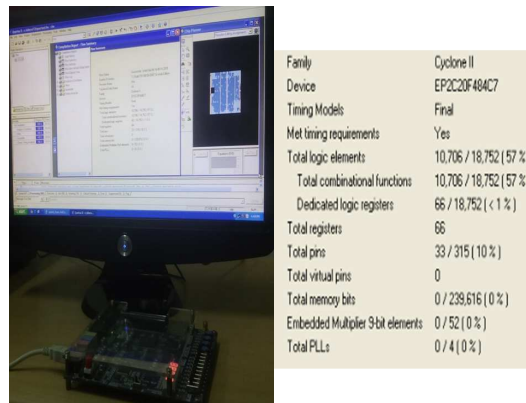


Figure 2: Left: Experimental setup for spatiotemporal pattern generation using FPGA. Right: Details of the components used.

The inclusion of two temporal signals, one each at $C(1)$ and $C(2)$ imply that two frequency ratios act as temporal rules and the $Nfactor$ acts as the spatial rule, along with setting the temporal ratios as $r_{C(1)} = 16.7MHz/12.5MHz$ and $r_{C(2)} = 16.7MHz/10MHz$.

The generated spatiotemporal patterns are illustrated for various temporal and spatial rules in Fig. (3). A study into the features exhibited by the spatiotemporal patterns reveal the following points:

1. Unlike conventional spatiotemporal pattern generations such as cellular automata, the proposed spatiotemporal patterns originate from a temporal basis rather than a spatial 'neighbourhood rule' [13]. This implies that the implementation is made extremely simple with no necessity of memory or lookup table required to store rules.
2. It is noted that as time progresses, the signal also spatially 'propagates' across various cells, truly testifying to the phrase 'spatio-temporal'.

3. On a similar note, it is also observed that at the $i-th$ cell, signal generation starts only when the Chaotic Signal originated from the first stages 'reaches' the $i-th$ stage. This is a highlight of the principle of causality.

4. On examination of the spatiotemporal patterns, one encounters multiple alternating regions of 'dark' and 'bright', with the bright signifying an absence of rich variations and dark signifying their presence. Thus, in essence, the 'bright' stages represent a subdued state of information, only to be conspicuously visible in later cells/time as a 'dark' pattern.

5. It is seen that, every time a 'dark' pattern arises out of the 'bright' subdued stage, it appears more diffused and spatially rich than the previous dark stage. This gives a clear insight into the pattern taken by the information in 'spreading'.

6. One observes that along any row or column, the patterns generated seldom repeat. This is a direct consequence of the ergodicity property of chaos.
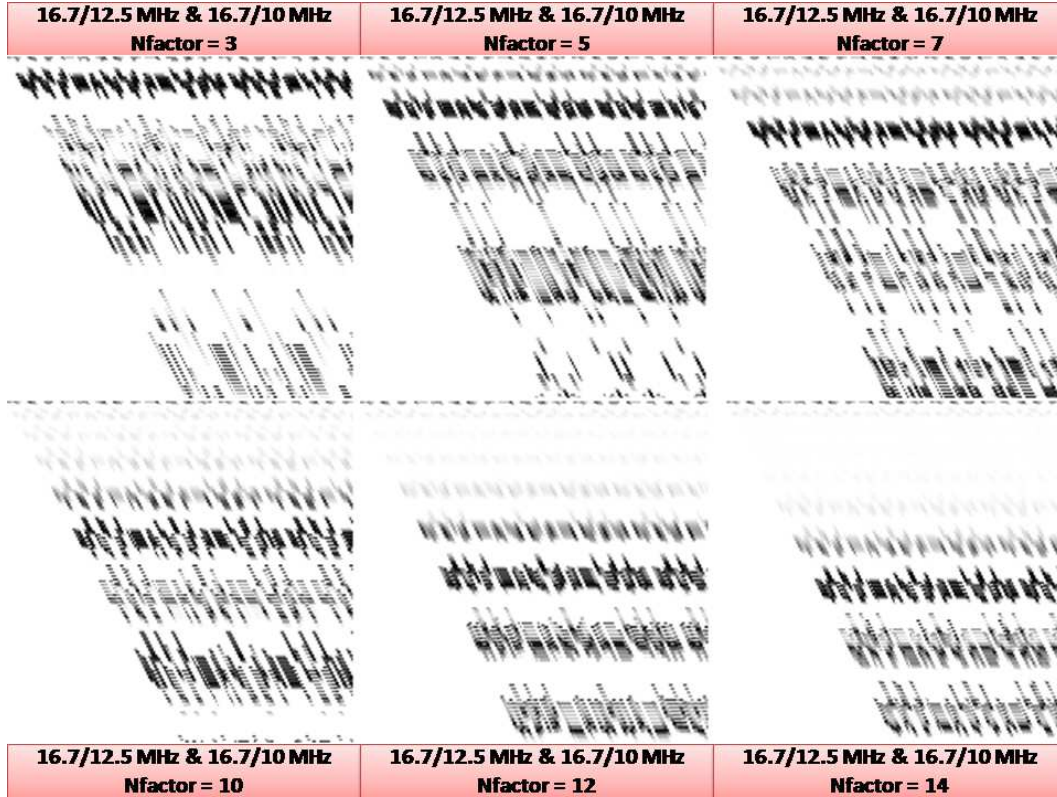


Figure 3: Spatiotemporal patterns generated for temporal ratios $r_{C(1)} = 16.7MHz/12.5MHz$ and $r_{C(2)} = 16.7MHz/10MHz$ and various $Nfactor$ values ranging from 3 to 14.

In the appendix/supplementary material, the time domain waveforms of all the 200 cells are plotted for a $Nfactor$ value of 5. From these waveforms the following conclusions can be obtained:

1. The initial 'bright' region of the spatiotemporal pattern correspond to the first 25-30 cells where nearly no significant features are observed.

2. Between the cell values of 30 and 45, we observe the formation of patterns. Of specific mention are the pulses being formed, comparable in principle to the creation of peregrine solitons and rogue waves [14].

3. From cells 45 to 55, it is observed that the pulses gain prominence, forming a specific repetitive '2 big + 1 small' pattern, reminiscent of the 'Three Sisters' formation.

4. In cells 55 to 100, one encounters a second 'bright' stage, where the features gradually decay into oblivion.

5. The cells from 100 to 115 show the regeneration of patterns, specifically in the form of dark pulses. The pulses become more pronounced in farther spatial cells.

6. One encounters an interesting wave-shaping activity between cells 115 to 150. Specifically, the crests of the dark pulses get narrower and troughs get wider, slowly transforming into bright pulses. Of noteworthy interest are the pulse compression of the bright pulses seen from cell 124 to cell 150.

4

7. The cells 150 to 200 give the impression of an anti-climactic extension to the interesting activity observed in the earlier cells. Specifically, the generated pulses slowly decay, pulses of much smaller amplitude are formed, and clumping of these pulses into another albeit much smaller 'three sisters' formation is observed [15].

In order to study the effect of $Nfactor$ on the spatiotemporal patterns, patterns obtained using the temporal ratios $r_{C(1)} = 16.7MHz/12.5MHz$ and $r_{C(2)} = 16.7MHz/10MHz$ and various $Nfactor$ values ranging from 3 to 14 are plotted in Fig. (3). The main inferences obtained from the figure are as follows:

1. As the value of $Nfactor$ increases the lengths of the 'dark' and 'bright' stages decrease, with the number of such dark and bright stages on the increase.
2. The initial 'bright' stage and subsequent 'regeneration' of the patterns become more pronounces at higher $Nfactor$ values.
3. The protrusions from the 'dark' stages to the bright ones are in the time domain, compressed pulses that carry the information of the patterns. This is reminiscent of the biological 'cocoon' stage of a larva where, all the necessary information and nutrition are compactly contained in a 'capsule' waiting for the metamorphic evolution into a full-fledged adult butterfly [16].

Finally, the effect of frequency on the formation of spatiotemporal patterns are investigated. Fig. (4) shows the spatiotemporal patterns obtained for various frequency ratios, maintaining a constant $Nfactor$ value of 5. The following points are inferred:

1. For a non-chaotic case, where $r_{C(1)}$ and $r_{C(2)}$ are set to 1, the significant lack of features and patterns are observed.
2. Since the $Nfactor$ is maintained constant, the spatial trend of the patterns with respect to the 'bright' and 'dark' stages remain the same.
3. However, there is a marked difference in the temporal characteristics of the spatiotemporal patterns generated, with the 'bunching' of features in the dark stages varying according to the frequency ratios chosen.
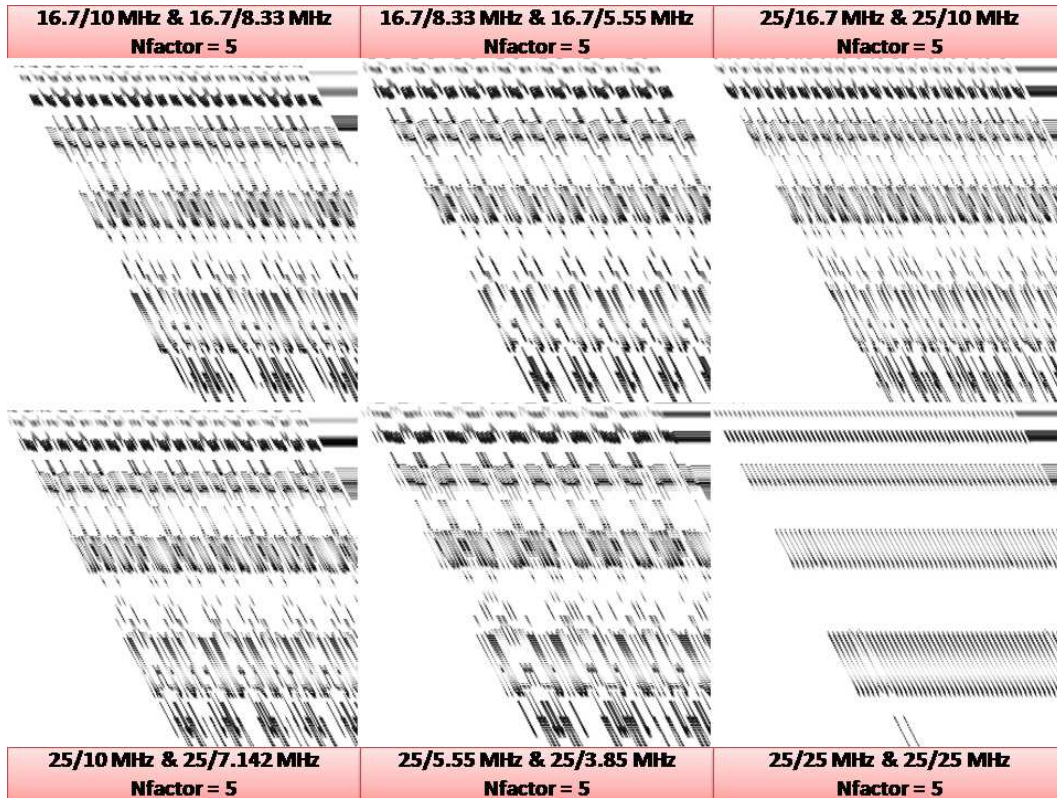


Figure 4: Spatiotemporal patterns generated for $Nfactor$ value of 5 and various temporal ratios.

At this juncture, it is noteworthy that tone observes the above mentioned features in the spatiotemporal patterns which are themselves generated by allowing the chaotic system described by the spatial and temporal rules to evolve naturally in a frequency dependent scenario. The extreme simplicity of the spatiotemporal pattern generator, combined with the rich variety of features observed form the pieces de resistance of the present work.

5

## 4. Conclusion

A novel kind of chaos - frequency dependant chaos is formulated and characterized using the iterative map, bifurcation diagrams and cobweb plots. It is seen that the proposal of a frequency dependant rather than amplitude dependant chaos promises two crucial advantages - easy tunability, thanks to the driving signals and simplicity of implementation. Experimental implementation of the generation of a temporal chaotic signal using the chaos formulation is carried out using FPGA and characterized using standard parameters such as Kolmogorov Entropy, Lyapunov Exponent and Fractal Dimension, following which the dependence of the nature of chaos into the driving frequency is studied. Based on these results, and the formulation of a spatial rule, the spatial propagation of the temporal signal generating spatiotemporal patterns are obtained. A feature study of the observed patterns is performed and the dependence of the generated patterns on the spatial and temporal 'rules' are investigated. The principal highlights of the spatiotemporal pattern generation are the richness of features obtained and the extreme simplicity with which these patterns are generated.

The generated spatiotemporal patterns find immense applications such as in 1D and 2D bar code generation and random number generation, which in turn are used in various secure communications and ciphering applications. The study into the features exhibited by such patterns facilitate a clear understanding into the nature of information creation and propagation in such media, and intelligent utilization of such knowledge could lead to secure compression of data with high compression ratios. Thus, the novel concept of frequency dependence and the richness of the spatiotemporal patterns generated using simple designs pave the way for affordable Big Data - a true testimony to the principle of 'Transformation through Information'.

## References

[1] G. B. Giannakis, F. Bach, R. Cendrillon, M. Mahoney,J. Neville, *Signal Processing for Big Data*, IEEE Signal Processing Magazine, **31**, 15-16 (2014).

[2] M. Hilbert, *How much of the global information and communication explosion is driven by more, and how much by better technology?*, Wiley Journal of the Association for Information Science and Technology, **65**, 856-861 (2014).

[3] M. Ausloos, M. Dirickx, *The Logistic Map and the Route to Chaos: From the Beginnings to Modern Applications*, (Springer, US, [2006]).

[4] S. H. Strogatz, *Nonlinear Dynamics and Chaos: With Applications to Physics, Biology, Chemistry, and Engineering* ,(Westview Press, Cambridge, 2008).

[5] E.Bilotta and P.Pantano, *A gallery of Chua attractors*, (World Scientific, Singapore, 2008).

[6] M. H. Jensen, P. Bak, T. Bohr, *Complete Devil's Staircase, Fractal Dimension, and Universality of Mode- Locking Structure in the Circle Map*, Phys. Rev. Lett. **50**, 1637 (1983).

[7] M. F. Barnsley, A. D. Sloan, *Chaotic Compression*, Computer Graphics World, **3** (1987).

[8] K. E. Barner and G. R. Arce, *Nonlinear Signal and Image Processing: Theory, Methods, and Applications*, (CRC Press, U.S, 2003).

[9] B. Razavi, *RF Microelectronics*, (Prentice Hall, US, 2011).

[10] R. G. James, K. Burke, J. P. Crutchfield, *Chaos forgets and remembers: Measuring information creation, destruction, and storage*, Int. J Bifurcation Chaos. **378**, 2124 (2014).

[11] M. T. Rosenstein, J. J. Collins, C. J. De Luca, *A practical method for calculating largest Lyapunov exponents from small data sets*, Physica D, **65**, 117, (1993).

[12] P. Maragos, F. K. Sun, *Measuring the fractal dimension of signals: morphological covers and iterative optimization*, IEEE Trans. Signal Processing, 41, 108-121 (1993).

[13] S. Wolfram, *A new kind of Science*, (Northwestern University Press, U.S, 2002).

[14] N. Akhmediev, J. M. S. Crespo and A. Ankiewicz, *Extreme waves that appear from nowhere: On the nature of rogue waves*, Phys. Lett. A, **373**, 2137, (2009).

[15] A. Ankiewics, D. J. Kedziora and N. Akhmediev, *Rogue wave triplets*, Phys. Lett. A, **375**, 2782, (2011).

[16] D. Abbott, P. C. W. Davies and A. K. Pati, *Quantum Aspects of Life*, (Imperial College Press, U.K, 2008).

## 5. Appendix

The following illustrate the temporal waveforms of a selection of the 200 spatial cells. The $N factor$ used is 5, and the frequency ratios for the first two cells are set as $r_{C(1)}$=16.7$MHz$/12.5$MHz$ and $r_{C(1)}$=16.7$MHz$/10$MHz$.
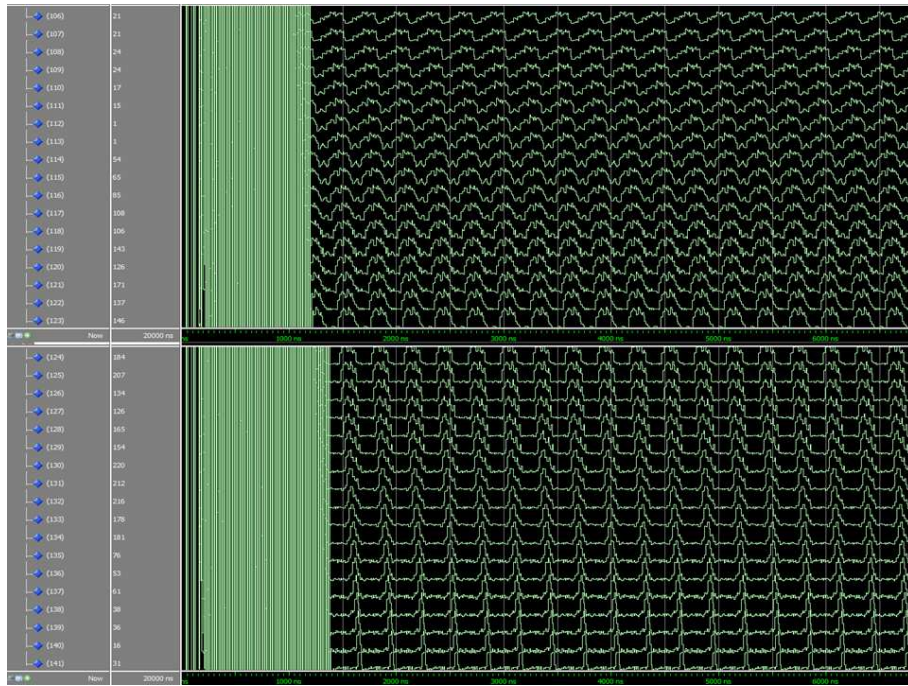
Figure 5: Temporal waveforms obtained for spatial cells - part 4.
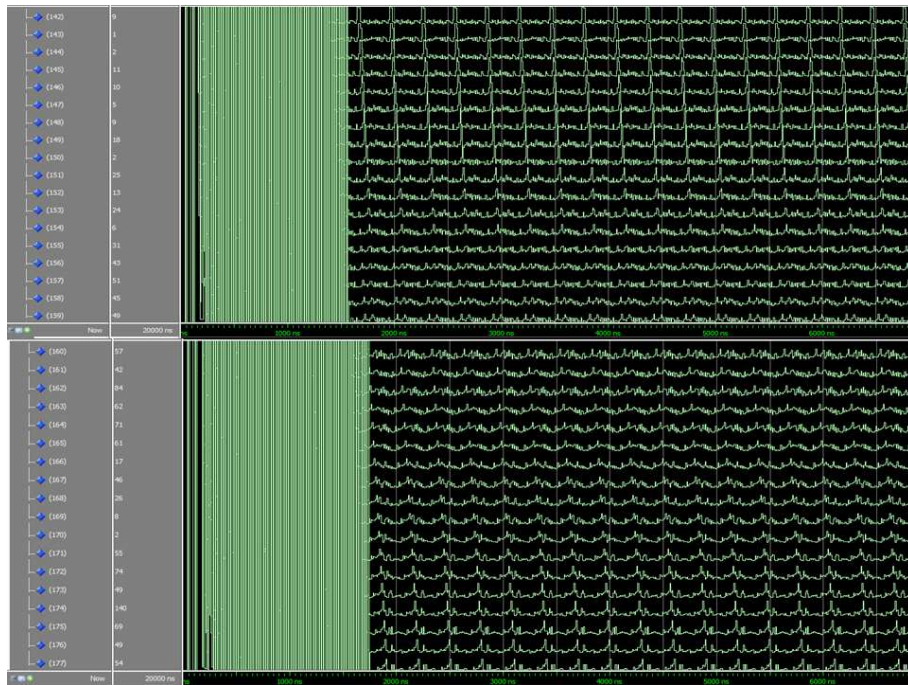


Figure 6: Temporal waveforms obtained for spatial cells - part 5.